CO Activation on the Late Lanthanide Dimers: Matrix Infrared Spectra of the Ln$_2$[η^2(μ_2-C, O)]$_x$ (Ln = Tb, Dy, Ho, Er, Lu; x = 1, 2) Molecules

Ling Jiang,[†] **Xi Jin,**[‡] **Mingfei Zhou,**[*,‡] **and Qiang Xu**[*,†]

National Institute of Advanced Industrial Science and Technology (AIST), Ikeda, Osaka 563-8577, Japan, and Department of Chemistry & Laser Chemistry Institute, Shanghai Key Laboratory of Molecular Catalysts and Innovative Materials, Fudan University, Shanghai 200433, Peoples Republic of China

Reactions of laser-ablated late lanthanide atoms (Tb, Dy, Ho, Er, Tm, Yb, and Lu) with dilute carbon monoxide molecules in solid argon have been investigated using matrix-isolation infrared spectroscopy. The Ln$_2$[η^2-(μ_2-C, O)]$_x$ (Ln = Tb, Dy, Ho, Er, Lu; x = 1, 2) molecules are observed upon sample annealing, whereas no product is observed for Tm and Yb. The C–O stretching frequencies in these dilanthanide carbonyls range from 1100 to 1300 cm^{-1}, far below the value of free CO in the gas phase (2143.5 cm^{-1}), implying that the C–O bonds are highly activated. Density functional theory calculations have been performed on these products. These Ln$_2$[η^2(μ_2-C, O)]$_x$ molecules are predicted to have planar structures, which carry asymmetrically bridging CO moieties that are tilted to the side.

Introduction

The study of carbon monoxide activation and reduction has gained considerable attention because of its importance in numerous industrial processes such as hydroformylation, alcohol synthesis, and acetic acid synthesis.[1,2] The interaction of metal atoms and small clusters with carbon monoxide serves as ideal models for fundamental understanding of the multifaceted mechanisms of carbon monoxide activation by metal complexes and surfaces. Reactions of various transition-metal and main-group metal atoms with carbon monoxide have been investigated, and a series of metal carbonyl complexes have been experimentally characterized.[3–5] Quantum chemical calculations have been performed to understand the electronic structures and bonding characteristics of metal carbonyl complexes.[3,4,6,7]

Recent matrix investigations have revealed that the monocarbonyls of Nb, Th, and U can be isomerized to the inserted carbide-oxide molecules on visible light irradiation.[8–10] The dicarbonyls of the Ti group, the V group, and the actinide metals Th and U undergo photoinduced isomerization to the OMCCO (M = Ti, Zr, Hf, V, Nb, Ta, U, and Th) molecules with visible or UV photons.[8–11] The OMCCO molecules can undergo further photochemical rearrangement to the OTh(η^3-CCO) or (η^2-C$_2$)-MO$_2$ (M = Nb, Ta, and U) molecules with UV photons. Furthermore, the OCBBCO molecule undergoes successive photochemical rearrangements to form the OBBCCO isomer and finally the OBCCBO molecule, which offers a novel example of CO dissociation by the main-group elements.[12] Interestingly, the reactions of CO with group 3 metal and early lanthanide dimers generated a new series of the M$_2$[η^2(μ_2-C, O)] (M = Sc, Y, La, Ce, Gd) molecules with asymmetrically bridging and side-on-bonded CO ligands, which are drastically activated with remarkably low C–O stretching frequencies.[13] A series of binary lanthanide metal carbonyls were prepared

and were characterized in rare-gas matrixes.[14] Here, we report a study of reactions of laser-ablated late lanthanide atoms (Tb–Lu) with carbon monoxide in excess argon. IR spectroscopy coupled with theoretical calculations provides evidence for the formation of the side-on-bonded Ln$_2$[η^2(μ_2-C, O)]$_x$ (Ln = Tb, Dy, Ho, Er, Lu; x = 1, 2) molecules, exhibiting unusually low C–O stretching frequencies ranging from 1100 to 1300 cm^{-1}, characteristic of anomalously weakened C–O bonds.

Experimental and Theoretical Methods

The experiment for laser ablation and matrix isolation infrared spectroscopy is similar to those previously reported.[15,16] In short, the Nd:YAG laser fundamental (1064 nm, 10 Hz repetition rate with 10 ns pulse width) was focused on the rotating late lanthanide (Tb, Dy, Ho, Er, Tm, Yb, and Lu) targets. The laser-ablated late lanthanide atoms were co-deposited with CO in excess argon onto a CsI window cooled normally to 4 K by means of a closed-cycle helium refrigerator. Typically, 1–18 mJ/pulse laser power was used. CO (99.95%), ^{13}C^{16}O (99%, ^{18}O < 1%), and ^{12}C^{18}O (99%) were used to prepare the CO/Ar mixtures. In general, matrix samples were deposited for 30 to 60 min with a typical rate of 2–4 mmol per hour. After sample deposition, IR spectra were recorded on a BIO-RAD FTS-6000e spectrometer at 0.5 cm^{-1} resolution using a liquid nitrogen cooled HgCdTe (MCT) detector for the spectral range of 5000–400 cm^{-1}. Samples were annealed at different temperatures and subjected to broad-band irradiation (λ > 250 nm) using a high-pressure mercury arc lamp (Ushio, 100 W).

Density functional theory (DFT) calculations were performed to predict the structures and vibrational frequencies of the observed reaction products using the Gaussian 03 program.[17] The BP86 and B3LYP density functional methods were used.[18] The Aug-cc-pVQZ basis set was used for the C and O atoms,[19] and the scalar-relativistic SDD pseudopotential and basis set were used for the late lanthanide atoms.[20] Geometries were fully optimized and vibrational frequencies were calculated with analytical second derivatives. Recent investigations have shown that computational methods, such as infrared frequencies,

* To whom correspondence should be addressed. E-mail: q.xu@aist.go.jp (Q.X.) and mfzhou@fudan.edu.cn (M.Z.).
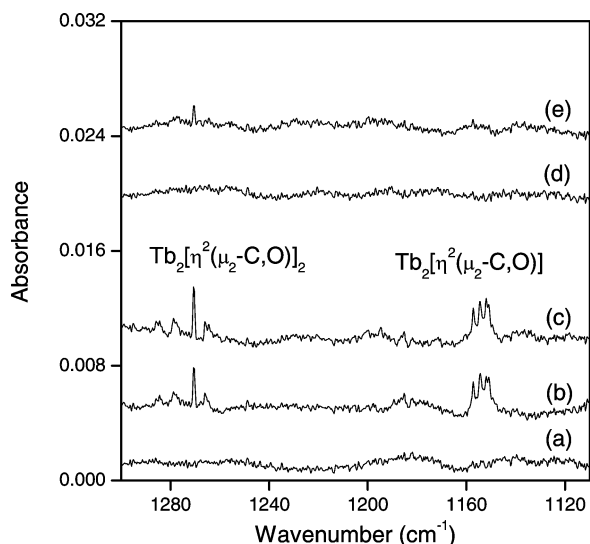† National Institute of Advanced Industrial Science and Technology.
‡ Fudan University.

Figure 1. IR spectra in the 1280−1120 cm^{-1} region for laser-ablated Tb atoms co-deposited with 0.06% CO in argon at 4 K: (a) 1 h of sample deposition, (b) after annealing to 30 K, (c) after annealing to 34 K, (d) after 20 min of broad-band irradiation, and (e) after annealing to 38 K.
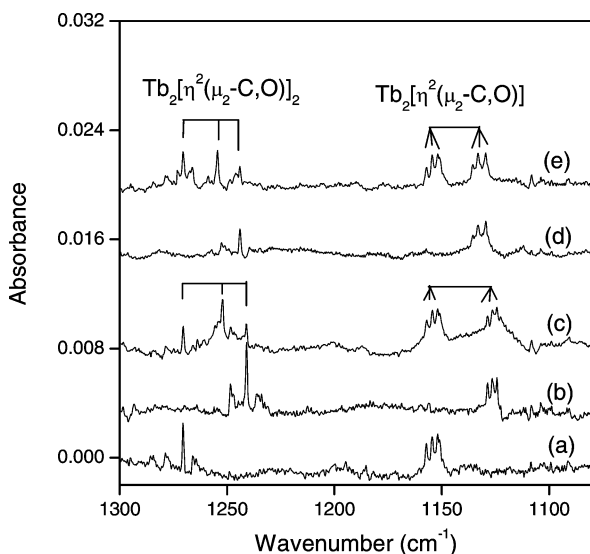

Figure 2. Infrared spectra in the 1300−1100 cm^{-1} region for laser-ablated Tb atoms co-deposited with isotopic CO in Ar for 1 h at 4 K, followed by annealing to 34 K: (a) 0.06% $^{12}C^{16}O$, (b) 0.06% $^{13}C^{16}O$, (c) 0.05% $^{12}C^{16}O$ + 0.05% $^{13}C^{16}O$, (d) 0.06% $^{12}C^{18}O$, and (e) 0.05% $^{12}C^{16}O$ + 0.05% $^{12}C^{18}O$.

relative absorption intensities, and isotopic shifts, can provide reliable information for lanthanide complexes.[13c,13d,21]

Results and Discussion

Experiments have been done with carbon monoxide concentrations ranging from 0.02% to 1.0% in excess argon. Mononuclear and dinuclear carbonyls are observed for Tb, Dy, Ho, Er, and Lu, but not for Tm and Yb. Considering that the isotopic splittings for some mononuclear carbonyls in the terminal C−O stretching frequency region cannot be well resolved because of band overlap, only the results of dinuclear carbonyls will be presented for discussion here. Typical infrared spectra for the reactions of laser-ablated late Tb dimers with CO molecules in excess argon in the selected regions are illustrated in Figures 1 and 2. The spectra of the other metals are shown as Supporting Information. The absorption bands in different isotopic experi-

TABLE 1: Infrared Absorptions (cm^{-1}) Observed for the Ln$_2$[$\eta^2(\mu_2$-C, O)]$_x$ (Ln = Tb, Dy, Ho, Er, Lu; x = 1, 2) Molecules in Solid Argon

$^{12}C^{16}O$	$^{13}C^{16}O$	$^{12}C^{18}O$	R(12/13)	R(16/18)	assignment
1270.5	1241.0	1244.0	1.0238	1.0213	Tb$_2$[$\eta^2(\mu_2$-C,O)]$_2$
1157.2	1128.6	1135.5	1.0253	1.0191	Tb$_2$[$\eta^2(\mu_2$-C,O)] site
1154.6	1126.4	1133.1	1.0250	1.0190	Tb$_2$[$\eta^2(\mu_2$-C,O)] site
1152.0	1124.3	1129.5	1.0246	1.0199	Tb$_2$[$\eta^2(\mu_2$-C,O)]
1277.6	1247.9	1251.1	1.0238	1.0212	Dy$_2$[$\eta^2(\mu_2$-C,O)]$_2$
1137.7	1110.7	1117.5	1.0243	1.0181	Dy$_2$[$\eta^2(\mu_2$-C,O)]
1119.2	1091.9	1098.5	1.0250	1.0188	Dy$_2$[$\eta^2(\mu_2$-C,O)] site
1269.8	1240.2	1243.6	1.0239	1.0211	Ho$_2$[$\eta^2(\mu_2$-C,O)]$_2$
1153.0	1123.9	1131.3	1.0259	1.0192	Ho$_2$[$\eta^2(\mu_2$-C,O)]
1265.7	1236.1	1239.8	1.0239	1.0209	Er$_2$[$\eta^2(\mu_2$-C,O)]$_2$ site
1256.8	1227.3	1231.4	1.0240	1.0206	Er$_2$[$\eta^2(\mu_2$-C,O)]$_2$
1140.6	1111.9	1120.5	1.0258	1.0179	Er$_2$[$\eta^2(\mu_2$-C,O)]
1121.2	1093.2	1102.7	1.0256	1.0168	Er$_2$[$\eta^2(\mu_2$-C,O)] site
1263.7	1234.0	1238.1	1.0241	1.0207	Lu$_2$[$\eta^2(\mu_2$-C,O)]$_2$
1100.7	1073.1	1081.8	1.0257	1.0175	Lu$_2$[$\eta^2(\mu_2$-C,O)]

TABLE 2: Comparison of Observed and Calculated IR Frequencies (cm^{-1}) for the Ln$_2$[$\eta^2(\mu_2$-C, O)]$_x$ (Ln = Tb, Dy, Ho, Er, Lu; x = 1, 2) Molecules

	Ln$_2$[$\eta^2(\mu_2$-C, O)]			Ln$_2$[$\eta^2(\mu_2$-C, O)]$_2$		
		Calcd			Calcd	
atom	obsd	BP86	B3LYP	obsd	BP86	B3LYP
Tb	1157.2	1309.2	1313.1	1270.5	1377.0	1330.9
Dy	1137.7	1500.8	1462.8	1277.6	1475.1	1531.9
Ho	1153.0	1525.3	1479.1	1269.8	1469.6	1495.8
Er	1140.6	1384.2	1508.1	1256.8	1363.8	1405.8
Lu	1100.7	1147.1	1168.2	1263.7	1363.9	1401.2

ments are listed in Table 1. The stepwise annealing and irradiation behavior of the product absorptions is also shown in the figures and will be discussed below.

Quantum chemical calculations have been carried out for the possible isomers and electronic states of the potential product molecules. The comparison of the observed and calculated IR frequencies is summarized in Table 2. Similar geometrical parameters of the reaction products have been obtained from both the BP86 and the B3LYP functionals, and the optimized structures are shown in Figure 3.

Ln$_2$[$\eta^2(\mu_2$-C, O)] (Ln = Tb, Dy, Ho, Er, Lu). Taking the Tb reaction as an example, the absorptions at 1157.2, 1154.6, and 1152.0 cm^{-1} appear on sample annealing, disappear after broad-band irradiation, and recover slightly upon further annealing to 38 K (Table 1 and Figure 1). On the basis of the growth/decay characteristics as a function of changes of experimental conditions, these three bands can be grouped together to one species. The main band of 1152.0 cm^{-1} shifts to 1124.3 cm^{-1} with $^{13}C^{16}O$ and shifts to 1129.5 cm^{-1} with $^{12}C^{18}O$, respectively (Table 1 and Figure 2, traces b and d), exhibiting isotopic frequency ratios ($^{12}C^{16}O/^{13}C^{16}O$, 1.0246; $^{12}C^{16}O/^{12}C^{18}O$, 1.0199) characteristic of C−O stretching vibrations. The unusually low C−O stretching frequency implies that the CO is side-on-bonded in this product. In the mixed $^{12}C^{16}O$ + $^{13}C^{16}O$ and $^{12}C^{16}O$ + $^{12}C^{18}O$ experiments (Figure 2, traces c and e), only pure isotopic counterparts are observed, indicating that only one CO subunit is involved.[22] Note that these new absorptions are only observed in the experiments with relatively lower CO concentration and higher laser power, indicating that the new products involve more than one Tb atom. Analogous to the M$_2$[$\eta^2(\mu_2$-C, O)] (M = Sc, Y, La, Ce, Gd) molecules,[13] the absorptions at 1157.2, 1154.6, and 1152.0 cm^{-1} are assigned to the C−O stretching modes of the Tb$_2$[$\eta^2(\mu_2$-C, O)] molecule in different matrix sites on the basis of the isotopic substitution and the CO concentration and laser power dependences of product yields.
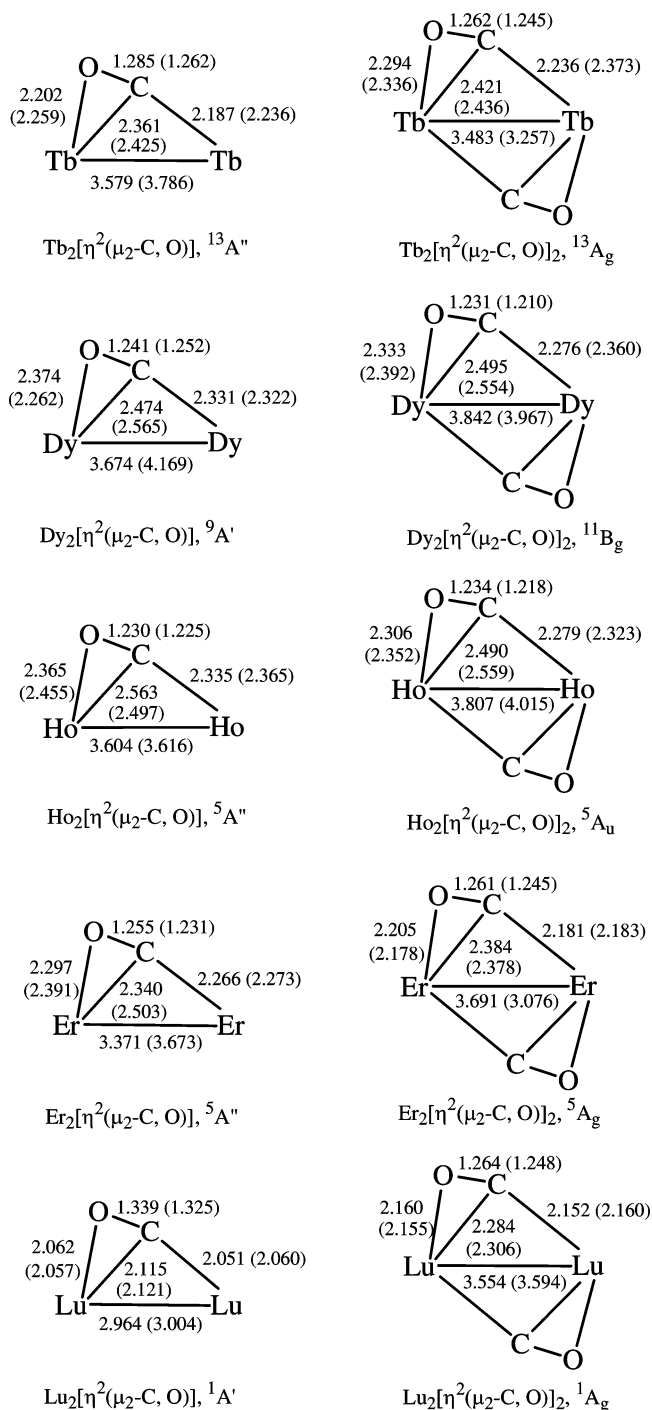
CO Activation on the Late Lanthanide Dimers

J. Phys. Chem. A, Vol. 112, No. 16, 2008 **3629**

Figure 3. Optimized structures (bond lengths in angstroms, bond angles in degrees) of the observed molecules with the BP86 and B3LYP (in parentheses) methods.

In the reactions of CO with Dy, Ho, Er, and Lu dimers, the absorptions of the analogous $Ln_2[\eta^2(\mu_2\text{-}C, O)]$ (Ln = Dy, Ho, Er, Lu) molecules have been observed in the region of 1100–1160 cm^{-1} (Dy, 1137.7, 1119.2; Ho, 1153.0; Er, 1140.6, 1121.2; Lu, 1100.7 cm^{-1}; Table 1 and Figures S1–S8 in Supporting Information).
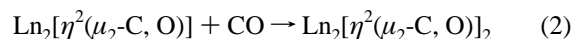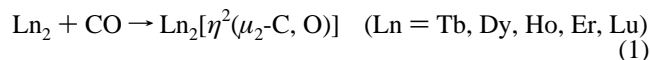
DFT calculations support the above assignments. The Ln_2-$[\eta^2(\mu_2\text{-}C, O)]$ (Ln = Tb, Dy, Ho, Er, Lu) molecules are predicted to have planar C_s structures with asymmetrically bridging and side-on-bonded CO ligands (Figure 3). The C atom is bonded to both Ln atoms with two inequivalent Ln–C bonds. The C–O bond lengths (1.225–1.325 Å) are very close to those of the analogous $M_2[\eta^2(\mu_2\text{-}C, O)]$ (M = Sc, Y, La, Ce, Gd) mol-

ecules,[13] which are much longer than the value of free CO in the gas phase (1.128 Å).[23] This suggests that the C–O bonds are activated in the $Ln_2[\eta^2(\mu_2\text{-}C, O)]$ (Ln = Tb, Dy, Ho, Er, Lu) molecules. The C–O stretching frequencies are calculated in the region of 1170–1480 cm^{-1} (Table 2), systematically higher than the observed values. The calculated $^{12}C^{16}O/^{13}C^{16}O$ and $^{12}C^{16}O/^{12}C^{18}O$ isotopic frequency ratios (not shown here) are consistent with the observed values. It is noted that the BP86 functional gives calculated C–O stretching vibrational frequencies slightly closer to the experimental values than the B3LYP functional as were found in many cases such as metal carbonyls.[3,4]

$Ln_2[\eta^2(\mu_2\text{-}C, O)]_2$ (Ln = Tb, Dy, Ho, Er, Lu). Under the experimental condition of relatively lower CO concentration and higher laser power, reactions of laser-ablated Tb, Dy, Ho, Er, and Lu atoms with CO molecules produce quite strong absorptions in the region of 1200–1300 cm^{-1} (Tb, 1270.5; Dy, 1277.6; Ho, 1269.8; Er, 1265.7, 1256.8; Lu, 1263.7 cm^{-1}; Table 1, Figures 1 and 2, and Figures S1–S8 in Supporting Information). These absorptions appear after sample annealing, disappear after broad-band irradiation, and recover slightly upon further annealing to 38 K. These absorptions are assigned to the $Ln_2[\eta^2\text{-}(\mu_2\text{-}C, O)]_2$ molecules. By taking the $Tb_2 + CO$ reaction as an example, the absorption at 1270.5 cm^{-1} shifts to 1241.0 with $^{13}C^{16}O$ and to 1244.0 cm^{-1} with $^{12}C^{18}O$ (Table 1 and Figure 2, traces b and d), respectively, exhibiting isotopic frequency ratios ($^{12}C^{16}O/^{13}C^{16}O$, 1.0238; $^{12}C^{16}O/^{12}C^{18}O$, 1.0213) characteristic of C–O stretching vibrations. Triplet band has been observed in the mixed $^{12}C^{16}O + ^{13}C^{16}O$ and $^{12}C^{16}O + ^{12}C^{18}O$ isotopic spectra (Figure 2, traces c and e), respectively, suggesting that two equivalent CO subunits are involved in each mode.[22] The 1270.5 cm^{-1} absorption is therefore assigned to the symmetric C–O stretching mode of the $Tb_2[\eta^2(\mu_2\text{-}C, O)]_2$ molecule.

The assignments are supported by DFT calculations. As shown in Figure 3, the $Ln_2[\eta^2(\mu_2\text{-}C, O)]_2$ molecules are predicted to have planar structures with C_{2h} symmetry, which carry two asymmetrically bridging CO moieties that are tilted to the side. It can be seen from Figure 3 that the C–O bond lengths in the $Ln_2[\eta^2(\mu_2\text{-}C, O)]_2$ molecules (1.210–1.248 Å) are slightly shorter than those in the $Ln_2[\eta^2(\mu_2\text{-}C, O)]$ molecules (1.225–1.325 Å), which is in accord with the relative higher C–O stretching frequencies in the $Ln_2[\eta^2(\mu_2\text{-}C, O)]_2$ molecules. The calculated C–O stretching frequencies (Table 2) are also systematically higher than the observed values.

Reaction Mechanism. On the basis of the behavior of sample annealing and irradiation, together with the observed species and calculated stable isomers, a plausible reaction mechanism can be proposed as follows. Under the present experimental conditions, laser-ablated late dilanthanide (Tb–Lu) molecules react with carbon monoxide molecules in the argon matrices to produce metal carbonyl species, whereas no new absorption is observed for the reactions of CO with Tm and Yb atoms. The $Ln_2[\eta^2(\mu_2\text{-}C, O)]_x$ (Ln = Tb, Dy, Ho, Er, Lu; x = 1, 2) molecules are formed upon sample annealing. These dilanthanide carbonyls are generated by the reactions of dilanthanide molecules with carbon monoxide in solid argon (reactions 1 and 2):

$$Ln_2 + CO \rightarrow Ln_2[\eta^2(\mu_2\text{-}C, O)] \quad (Ln = Tb, Dy, Ho, Er, Lu) \tag{1}$$

$$Ln_2[\eta^2(\mu_2\text{-}C, O)] + CO \rightarrow Ln_2[\eta^2(\mu_2\text{-}C, O)]_2 \tag{2}$$

One of the most interesting findings of the present investigations is the observation of the side-on-bonded $Ln_2[\eta^2(\mu_2\text{-}C, O)]_x$ (Ln = Tb, Dy, Ho, Er, Lu; x = 1, 2) molecules. The C–O

stretching frequencies in these dilanthanide mono- and dicarbonyls range from 1100 to 1300 cm^{-1}, far below the value of free CO in the gas phase (2143.5 cm^{-1}),[23] implying that the C−O bonds are highly activated. Anomalous C−O bond weakening has been reported for chemisorbed CO in side-on-bonded modes on transition metal surfaces as model catalysts, for which the ν_{C-O} values were observed around 1100−1400 cm^{-1}.[24] Thus, the present findings together with the recent observations of M$_2$[η^2(μ_2-C, O)] (M = Sc, Y, La, Ce, Gd) molecules provide important information of structural configuration for CO activation on metal catalytst.[24]

Conclusions

Reactions of laser-ablated late lanthanide (Tb, Dy, Ho, Er, Tm, Yb, and Lu) atoms with dilute carbon monoxide molecules in solid argon have been investigated using matrix-isolation infrared spectroscopy. Dilanthanide carbonyls, Ln$_2$[η^2(μ_2-C, O)]$_x$ (x = 1, 2), are observed for Tb, Dy, Ho, Er, and Lu after sample annealing, but no carbonyl compounds are observed for Tm and Yb. These molecules exhibit unusually low C−O stretching frequencies ranging from 1100 to 1300 cm^{-1}, characteristic of anomalously weakened C−O bonds. Density functional theory calculations have been performed on these dilanthanide mono- and dicarbonyls, which support the identifications of these molecules from the matrix infrared spectra.

Supporting Information Available: The infrared spectra of the Dy, Ho, Er, and Lu reactions. This information is available free of charge via the Internet at http://pubs.acs.org.

References and Notes

(1) Cotton, F. A.; Wilkinson, G.; Murillo, C. A.; Bochmann, M. *Advanced Inorganic Chemistry*, 6th ed.; Wiley: New York, 1999.

(2) Muetterties, E. L.; Stein, J. *Chem. Rev.* **1979**, *79*, 479.

(3) Zhou, M. F.; Andrews, L.; Bauschlicher, C. W., Jr. *Chem. Rev.* **2001**, *101*, 1931, and references therein.

(4) Himmel, H. J.; Downs, A. J.; Greene, T. M. *Chem. Rev.* **2002**, *102*, 4191, and references therein.

(5) Xu, Q. *Coord. Chem. Rev.* **2002**, *231*, 83, and references therein.

(6) Frenking, G.; Frohlich, N. *Chem. Rev.* **2000**, *100*, 717, and references therein.

(7) Bridgeman, A. J. *Inorg. Chim. Acta.* **2001**, *321*, 27.

(8) Zhou, M. F.; Andrews, L. *J. Phys. Chem. A* **1999**, *103*, 7785.

(9) Zhou, M.; Andrews, L.; Li, J.; Bursten, B. E. *J. Am. Chem. Soc.* **1999**, *121*, 12188. Li, J.; Bursten, B. E.; Zhou, M. F.; Andrews, L. *Inorg. Chem.* **2001**, *40*, 5448.

(10) Zhou, M.; Andrews, L.; Li, J.; Bursten, B. E. *J. Am. Chem. Soc.* **1999**, *121*, 9712.

(11) Zhou, M. F.; Andrews, L. *J. Am. Chem. Soc.* **2000**, *122*, 1531.

(12) Zhou, M. F.; Tsumori, N.; Li, Z.; Fan, K.; Andrews, L.; Xu, Q. *J. Am. Chem. Soc.* **2002**, *124*, 12936. Zhou, M. F.; Jiang, L.; Xu, Q. *Chem. Eur. J.* **2004**, *10*, 5817.

(13) (a) Jiang, L.; Xu, Q. *J. Am. Chem. Soc.* **2005**, *127*, 42. (b) Jiang, L.; Xu, Q. *J. Phys. Chem. A* **2006**, *110*, 5636. (c) Xu, Q.; Jiang, L.; Zou, R. Q. *Chem. Eur. J.* **2006**, *12*, 3226. (d) Zhou, M. F.; Jin, X.; Li, J. *J. Phys. Chem. A* **2006**, *110*, 10206. (e) Jin, X.; Jiang, L.; Xu, Q.; Zhou, M. F. *J. Phys. Chem. A* **2006**, *110*, 12585.

(14) Slater, J. L.; Sheline, R. K.; Lin, K. C.; Weltner, W., Jr. *J. Chem. Phys.* **1971**, *55*, 5129. Slater, J. L.; DeVore, T. C.; Calder, V. *Inorg. Chem.* **1973**, *12*, 1918. Slater, J. L.; DeVore, T. C.; Calder, V. *Inorg. Chem.* **1974**, *13*, 1808. Sheline, R. K.; Slater, J. L. *Angew. Chem., Int. Ed. Engl.* **1975**, *14*, 309.

(15) Burkholder, T. R.; Andrews, L. *J. Chem. Phys.* **1991**, *95*, 8697.

(16) Zhou, M. F.; Tsumori, N.; Andrews, L.; Xu, Q. *J. Phys. Chem. A* **2003**, *107*, 2458. Jiang, L.; Xu, Q. *J. Chem. Phys.* **2005**, *122*, 034505. Jiang, L.; Teng, Y. L.; Xu, Q. *J. Phys. Chem. A* **2006**, *110*, 7092.

(17) Frisch, M. J.; Trucks, G. W.; Schlegel, H. B.; Scuseria, G. E.; Robb, M. A.; Cheeseman, J. R.; Montgomery, J. A., Jr.; Vreven, T.; Kudin, K. N.; Burant, J. C.; Millam, J. M.; Iyengar, S. S.; Tomasi, J.; Barone, V.; Mennucci, B.; Cossi, M.; Scalmani, G.; Rega, N.; Petersson, G. A.; Nakatsuji, H.; Hada, M.; Ehara, M.; Toyota, K.; Fukuda, R.; Hasegawa, J.; Ishida, M.; Nakajima, T.; Honda, Y.; Kitao, O.; Nakai, H.; Klene, M.; Li, X.; Knox, J. E.; Hratchian, H. P.; Cross, J. B.; Adamo, C.; Jaramillo, J.; Gomperts, R.; Stratmann, R. E.; Yazyev, O.; Austin, A. J.; Cammi, R.; Pomelli, C.; Ochterski, J. W.; Ayala, P. Y.; Morokuma, K.; Voth, G. A.; Salvador, P.; Dannenberg, J. J.; Zakrzewski, V. G.; Dapprich, S.; Daniels, A. D.; Strain, M. C.; Farkas, O.; Malick, D. K.; Rabuck, A. D.; Raghavachari, K.; Foresman, J. B.; Ortiz, J. V.; Cui, Q.; Baboul, A. G.; Clifford, S.; Cioslowski, J.; Stefanov, B. B.; Liu, G.; Liashenko, A.; Piskorz, P.; Komaromi, I.; Martin, R. L.; Fox, D. J.; Keith, T.; Al-Laham, M. A.; Peng, C. Y.; Nanayakkara, A.; Challacombe, M.; Gill, P. M. W.; Johnson, B.; Chen, W.; Wong, M. W.; Gonzalez, C.; Pople, J. A. *Gaussian 03*, revision B.04; Gaussian, Inc.: Pittsburgh, PA, 2003.

(18) Lee, C.; Yang, E.; Parr, R. G. *Phys. Rev. B* **1988**, *37*, 785. Becke, A. D. *J. Chem. Phys.* **1993**, *98*, 5648.

(19) Dunning, T. H., Jr. *J. Chem. Phys.* **1989**, *90*, 1007. Kendall, R. A.; Dunning, T. H., Jr.; Harrison, R. J. *J. Chem. Phys.* **1992**, *96*, 6796.

(20) Dolg, M.; Stoll, H.; Preuss, H. *J. Chem. Phys.* **1989**, *90*, 1730. Cao, X.; Dolg, M. *J. Chem. Phys.* **2001**, *115*, 7348.

(21) Xu, J.; Zhou, M. F. *J. Phys. Chem. A* **2006**, *110*, 10575. Xu, J.; Jin, X.; Zhou, M. F. *J. Phys. Chem. A* **2007**, *111*, 7105.

(22) Darling, J. H.; Ogden, J. S. *J. Chem. Soc., Dalton Trans.* **1972**, 2496.

(23) Huber, H.; Herzberg, G. *Constants of Diatomic Molecules*, Van Nostrand Reinhold: New York, 1979.

(24) Hoffmann, F. M.; de Paola, R. A. *Phys. Rev. Lett.* **1984**, *52*, 1697. Sinn, N. D.; Madey, T. E. *Phys. Rev. Lett.* **1984**, *53*, 2481. Moon, D. W.; Bernasek, S. L.; Dwyer, D. J.; Gland, J. L. *J. Am. Chem. Soc.* **1985**, *107*, 4363.